




Article

Development of Semisynthetic Apoptosis-Inducing Agents Based on Natural Phenolic Acids Scaffold: Design, Synthesis and In-Vitro Biological Evaluation

Shahira M. Ezzat ^{1,2}, Heba El Sayed Teba ³, Inas G. Shahin ³ , Ahmed M. Hafez ⁴ , Aliaa M. Kamal ^{3,5,*} and Nora M. Aborehab ⁶ 

¹ Pharmacognosy Department, Faculty of Pharmacy, Cairo University, Cairo 11562, Egypt

² Pharmacognosy Department, Faculty of Pharmacy, October University for Modern Sciences and Arts (MSA), Giza 12451, Egypt

³ Organic Chemistry Department, Faculty of Pharmacy, October University for Modern Sciences and Arts (MSA), Giza 12451, Egypt

⁴ Department of Biochemistry, School of Life and Medical Sciences, University of Hertfordshire Hosted by Global Academic Foundation, Cairo 11586, Egypt

⁵ Pharmaceutical Organic Chemistry Department, Faculty of Pharmacy, Cairo University, Cairo 11562, Egypt

⁶ Biochemistry Department, Faculty of Pharmacy, October University for Modern Sciences and Arts (MSA), Giza 12451, Egypt

* Correspondence: aliaa.kamal@pharma.cu.edu.eg or alkamal@msa.edu.eg

Abstract: A crucial target in drug research is magnifying efficacy and decreasing toxicity. Therefore, using natural active constituents as precursors will enhance both safety and biological activities. Despite having many pharmacological activities, caffeic and ferulic acids showed limited clinical usage due to their poor bioavailability and fast elimination. Therefore, semisynthetic compounds from these two acids were prepared and screened as anticancer agents. In this study, CA and FA showed very potent anticancer activity against Caco-2 cells. Consequently, eighteen derivatives were tested against the same cell line. Four potent candidates were selected for determination of the selectivity index, where compound **10** revealed a high safety margin. Compound **10** represented a new scaffold and showed significant cytotoxic activity against Caco-2. Cell-cycle analysis and evaluation of apoptosis showed that derivatives **10**, **7**, **11**, **15** and **14** showed the highest proportion of cells in a late apoptotic stage.

Keywords: anti-proliferative activity; synthesis; anticancer activity; cancer cell lines; drug discovery; semisynthetic amides; apoptosis inducer agents; Caco-2 cell line; matrix metalloproteinases



Citation: Ezzat, S.M.; Teba, H.E.S.; Shahin, I.G.; Hafez, A.M.; Kamal, A.M.; Aborehab, N.M. Development of Semisynthetic Apoptosis-Inducing Agents Based on Natural Phenolic Acids Scaffold: Design, Synthesis and In-Vitro Biological Evaluation. *Molecules* **2022**, *27*, 6724. <https://doi.org/10.3390/molecules27196724>

Academic Editor: Małgorzata Jelen

Received: 13 September 2022

Accepted: 4 October 2022

Published: 9 October 2022

Publisher's Note: MDPI stays neutral with regard to jurisdictional claims in published maps and institutional affiliations.



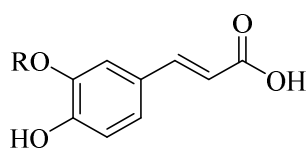
Copyright: © 2022 by the authors. Licensee MDPI, Basel, Switzerland. This article is an open access article distributed under the terms and conditions of the Creative Commons Attribution (CC BY) license (<https://creativecommons.org/licenses/by/4.0/>).

1. Introduction

Cancer has the highest social and economic burden among all human diseases, and coupled with that, in the coming four decades it is anticipated to leap from the second to the first place to become the leading cause of death worldwide [1].

Over the years, several natural anticancer molecules were used as scaffolds for the synthesis of anticancer drugs, such as vinblastine and vincristine from *Catharanthus* alkaloids [2], paclitaxel from Yew trees [3], and podophyllotoxin from *Podophyllum* resins [4].

Natural phenolic compounds are an important class of substances of plant origin that have both anticancer and anti-oxidant activities [5–8]. For this reason, new methods of their functionalization are developed to increase their application in medicine. Two of the most prevailing phenolic compounds are caffeic acid (CA) and ferulic acid (FA) (Figure 1).



R= H Caffeic acid (1)
 R= CH₃ Ferulic acid (2)

Figure 1. Structure of Caffeic acid and Ferulic acid.

Caffeic acid and its different derivatives were reported to possess many biological activities such as immunostimulants [9–12], antibacterial [13,14], anti-inflammatory [15], cardio protective [15,16], anti-atherosclerotic [9,17], antidiabetic [15,18], antiproliferative [19,20], hepatoprotective [21], anticancer [9,13–15,22–24], and Alzheimer’s disease [25].

Ferulic acid has been used in healthy food and nutrition restoratives due to its well-known antioxidant properties, and due to this biological effect, it can be used in Alzheimer’s disease [25,26]. It is highly recommended for diabetic patients [27]. Moreover, FA has a reported neuroprotective effect [28–30] and relieves ischemia-reperfusion-induced cell apoptosis [31,32]. FA also has a chemo-preventive activity against carcinogenesis induced by 7,12-dimethylbenz[*a*]anthracene (DMBA) in rats [33,34]. Equally important is its antiproliferative action on osteosarcoma cells where it induces apoptosis by blocking the PI3K/Akt pathway [35].

It is highly recommended for diabetic patients as it can alleviate oxidative stress and also has an antihyperglycemic effect. [27]

Recently, several phenolic compounds were tested against a spectrum of severe pathological conditions and both CA and FA showed potential results against coronavirus-based infections [36].

The aforementioned biological activities are achieved through a variety of mechanisms; the anticancer activity of both CA and FA is exerted by two mechanisms, acting as primary antioxidants that eliminate reactive oxygen species (ROS) and as secondary antioxidants (pro-oxidants) preventing the splitting of peroxides by metal ion chelation (iron and copper) [37,38]. Thus, inhibiting oxidative degradation of essential biological molecules (lipids, amino acids, polyunsaturated fatty acids and DNA bases) and preventing the formation of cellular lesions [25,39–42].

As antioxidants, the study of the structure activity relationship of both acids and their derivatives showed that the hydroxy groups in caffeic and ferulic acids proved to be a prerequisite for anti-oxidant activity, through their free radical scavenging and metal chelation properties. The 4-hydroxy moiety supports the resonance around the whole molecule resulting in higher stability due to the formation of the phenoxy radical. It is also accepted that a second 3-hydroxy substitution in caffeic acid promotes the antioxidant quality due to the formation of a stable ortho-quinone structure. Equally, in ferulic acid, the methoxy group enhances the resonance of the aromatic ring due to its electron-donating attributes. The acids have an additional aspect where the COOH tail provides lipid support and resonates with its neighboring unsaturation, offering alternative sites to prevent membrane deterioration by free radicals while the inclusion of H-donating groups in the side chain such as amide moiety accelerates the activity [43–45] (Figure 2).

As cell apoptosis promoters, it was established that CA and FA play a distinctive role in encouraging cell apoptosis in human cervical cancer cells through inhibition of the Bcl-2 activity [46,47] and in non-small lung cancer cells (NSCLC) through the MAPK pathway [48]

In another pathway, it was observed that the acids are responsible for suppressing hepatocellular carcinoma cells (HCC) via inhibiting the expression of vascular endothelial growth factor (VEGF), which in turn impedes angiogenesis of the tumor cells [49].

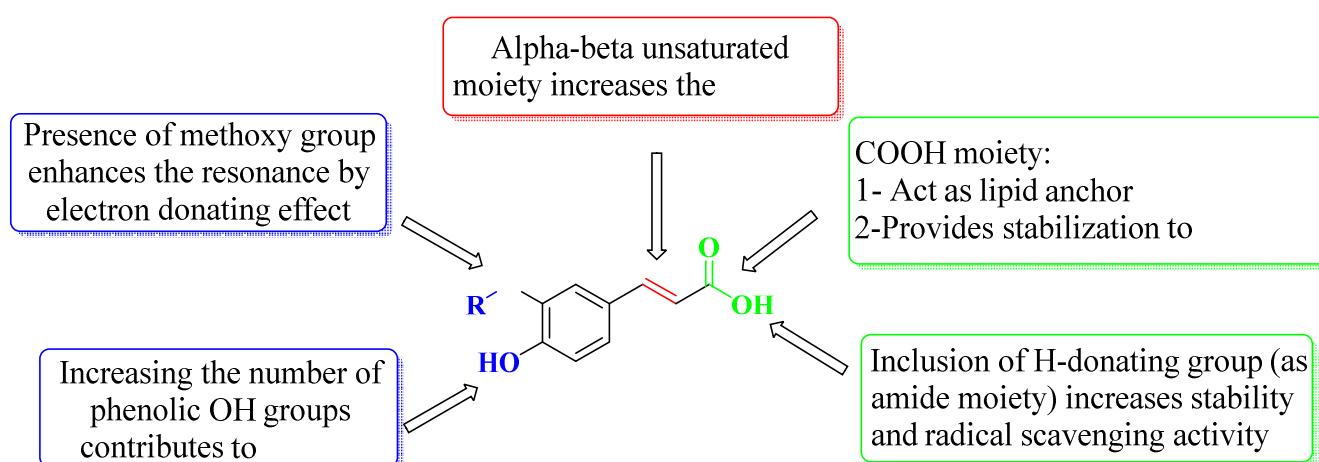


Figure 2. SAR of caffeic acid and ferulic acid as antioxidants.

It is worth mentioning that both CA and FA are highly selective, imparting cytotoxicity to tumor cells but not to normal cells; on the other hand, they are highly metabolized in the body, therefore jeopardizing their stability. By evaluating the two major derivatives—amides and esters—the amides possessed potent cytotoxic activity in addition to high in-vivo stability when put in comparison with the ester derivatives. Following in the same vein, 18 amide compounds (Table 1) were synthesized (Figure 3) via reacting the respective phenolic acids with a panel of amines, adopting *N,N'*-dicyclohexylcarbodiimide (DCC) as a coupling agent.

Table 1. Detailed structure of the semi synthesized compounds 3–20.

Cpd. No.	R	R ¹	Cpd. No.	R	R ¹
3	H		12	CH ₃	
4	H		13	CH ₃	
5	H		14	CH ₃	
6	H		15	CH ₃	
7	H		16	CH ₃	
8	H		17	CH ₃	
9	H		18	CH ₃	

Table 1. Cont.

Cpd. No.	R	R ¹	Cpd. No.	R	R ¹
10	H		19	CH ₃	
11	H		20	CH ₃	

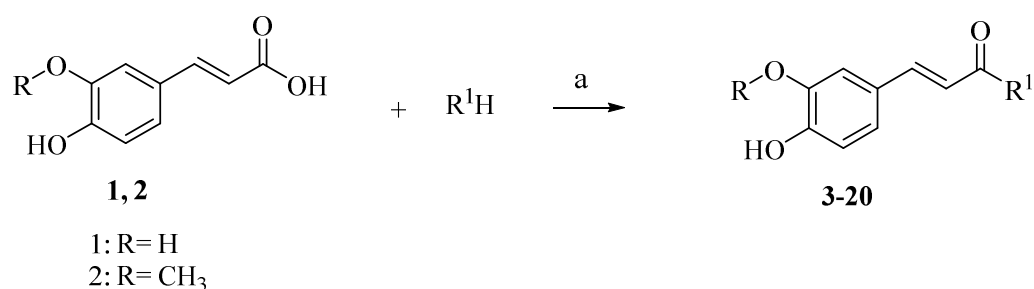


Figure 3. Scheme for the preparation of the candidate compounds.

Therefore, the current study was conducted to verify the anti-tumor activity of CA and FA versus their semisynthetic derivatives on different cell lines and explore the underlying mechanisms using the following scheme:

2. Results and Discussion

2.1. Chemistry

The synthesis of CA and FA derivatives **3–20** is displayed in Figure 3. Preparation of these candidates was carried out by reacting the naturally obtained caffeic or ferulic acids with different amines using *N,N'*-dicyclohexylcarbodiimide (DCC) as a coupling agent for the preparation of the amide linkage starting from the acids. Separated amides **3–20** were purified by column chromatography. The main idea is screening the effect of changing the alkyl/cycloalkyl/aralkyl/aryl/heterocyclic moiety of the amide functionality on the biological activity. Compounds **1** and **2** exhibited a sky-blue color in UV, which turns to a greenish yellow color on exposure to ammonia vapor and spraying with AlCl₃, indicating that they are phenolic acid in nature. ¹H NMR spectrum of **1** showed the characteristic signals for caffeic acid [50], which was characterized by two trans-olefinic protons at δ 6.16 and δ 7.41 ppm with a large coupling constant δ 15.88 Hz, assigned to H-8 and H-7, respectively. An ABX system was displayed at δ 6.76, 6.95 and δ 7.04 ppm assigned to H-5, H-6 and H-2, respectively. The ¹³C NMR showed the nine characteristic carbon signals for 3,4-dihydroxy trans cinnamic acid with two oxy carbons at δ 146.0 and δ 148.5 (C-3 and 4), one carbonyl carbon at δ 168.3 (C-9), two trans olefinic carbons at δ 145.07 and δ 115.5 ppm, in addition to C-1 at δ 126.1, C-2 at δ 115.1, C-5 at δ 116.2 and C-6 at δ 21.6. ¹H NMR spectrum of **2** showed the characteristic signals for ferulic acid [51], which was characterized by two trans-olefinic protons at δ 6.35 and 7.48 ppm with large coupling constant 15.88 Hz, assigned to H-8 and H-7, respectively. An ABX system was affirmed by these signals at δ 6.79, 7.07 and 7.28 ppm, corresponding to H-5, H-6 and H-2, respectively. The methoxy group at C-3 was manifested by the singlet signal at δ 3.82 ppm and integrated as three protons (Supporting Information).

The ¹³C-NMR supported the nine characteristic carbon signals for 4-Hydroxy-3-methoxycinnamic acid with two oxy carbons at δ 148.3 and 149.5 ppm (C-3 and C- 4), one carbonyl carbon at 168.4 ppm (C-9), two trans olefinic carbons at δ 144.9 and δ 115.9 ppm

and finally, C-1, C-2, C-5 and C-6 were confirmed by signals at δ 126.2, 111.6, 116.0 and 123.2 ppm respectively.

Reacting **1** and **2** with either phenyl piperazine, cyclohexyl amine, aromatic amines or aralkyl amine in presence of DCC afforded compounds **3**, **12**, **6**, **15**, **4**, **5**, **7**, **8**, **10**, **11**, **13**, **14**, **16**, **17**, **19**, **20**, **9** and **18** sequentially. The structures of these compounds were elucidated using spectral data and microanalyses.

IR spectra of all the candidates showed the characteristic carbonyl band of amide between 1626–1662 cm^{-1} while the NH band appeared in the range of 3510–3240 cm^{-1} for all compounds except **3** and **12**, which are tertiary amides. ^1H NMR spectra of compounds **3–20** exhibited the appearance of the doublet signal of HC=CH in the range of δ 5.70–7.73 ppm with large coupling constant 15.00–15.90 Hz. Compounds **3** and **12** revealed the multiplet signals in their ^1H NMR spectra at δ 1.04–1.85 ppm assigned to CH_2 of piperazine ring. ^1H NMR spectra of compounds **5**, **14** and **17** showed a series of singlet signals in the range of δ 2.26–2.29 ppm due to CH_3 group while the 11 protons corresponding to the cyclohexyl group in compounds **6** and **15** were confirmed by the appearance of multiplet signals in the range of δ 1–3.35 ppm. Compound **8** was the only CA derivative that showed a singlet signal corresponding to OCH_3 group at δ 3.63 ppm while **16** showed an additional OCH_3 group at δ 3.81 ppm. The appearance of singlet signals at δ 5.59 and 3.19 ppm in ^1H NMR spectra of **9** and **18** respectively confirmed the presence of N- CH_2 (Supporting Information). Compounds **11** and **20** revealed the presence of NH_2 group at δ 9.17 and 4.94 ppm, respectively. ^{13}C NMR spectrum of all compounds confirmed the presence of the characteristic C=O group, showing signals in the range of δ 160.7–170.9 ppm.

2.2. Biological Activity

2.2.1. Cell Viability Determination by MTT Assay

The cytotoxicity of the parent compounds **1** and **2** was tested against breast (MCF-7), liver (HepG2), lung epithelial (A459), colorectal (Caco-2) and pancreatic (PANC-1) cancer cell lines. Their cytotoxicity was compared to doxorubicin (DOX) and their selectivity was tested on Vero cells (Table 2). The cytotoxicity of both **1** and **2** was lower than that of DOX but the selectivity index (SI) was significantly higher than DOX (Supporting Information).

Table 2. IC_{50} of the parent compounds and doxorubicin on different cancer cell lines. Results are the average of triplicates.

Cpd. No.	IC_{50} (μM) \pm SD					SI *
	MCF-7	HepG2	A549	Caco-2	PANC-1	
Caffeic acid (1)	0.97 \pm 6.27	1.03 \pm 12.63	1.63 \pm 15.56	0.41 \pm 3.3	1.29 \pm 12.16	0.90
Ferulic acid (2)	1.12 \pm 10.15	0.81 \pm 2.17	1.74 \pm 10.8	0.41 \pm 1.92	1.08 \pm 2.27	1.08
Doxorubicin	0.17 \pm 2.00	0.18 \pm 3.4	0.14 \pm 1.3	0.17 \pm 1.1	0.16 \pm 1.86	0.04

* SI (Selectivity index) = IC_{50} on Vero cells/ IC_{50} on cancer cells.

Caco-2 showed the highest sensitivity to both acids **1** and **2** (IC_{50} = 0.41 μM for both caffeic and ferulic acids) and thus it was selected for testing the cytotoxicity of the 18 semisynthetic candidates. All the synthesized amides were far more potent than the parent acids by 10-fold or more with a slight reduction in the SI of these derivatives (Table 3). It is worth mentioning that caffeic acid derivatives were more potent than ferulic acid derivatives. Among the CA amide derivatives **3–11**, compound **10** was the most potent against the Caco-2 cancer cell line with an IC_{50} of 0.009 \pm 0.09 μM with a SI 14-fold greater than its IC_{50} followed by compounds **11**, **7** and **9** with an IC_{50} of 0.01 \pm 0.11, 0.02 \pm 0.11 and 0.03 \pm 0.29 μM , respectively. The potency of the rest of the CA amide derivatives ranged from IC_{50} = 0.05 μM to 0.08 μM , which was still much more potent than the parent acid. Regarding the FA amide derivatives **12–20**, compound **20** revealed the highest potency with an IC_{50} of 0.01 \pm 0.63 μM followed by compounds **15**, **17** and **19** with IC_{50} of 0.02 \pm 0.17,

0.02 ± 0.21 and 0.02 ± 0.65 µM sequentially. Moreover, compounds **12**, **13**, **14**, **16** and **18** showed very good cytotoxicity against Caco-2 with an IC₅₀ ranging from 0.04 µM to 0.08 µM. The derivatives were much more potent than the parent acid with an excellent SI (Table 3). To further confirm this, cell-cycle analysis and apoptosis assays were performed and the gene expression of p53, caspase 3, Bax, MMP-2 and MMP-9 was quantified.

Table 3. IC₅₀ of the semi-synthesized compounds on Caco-2 cancer cell line and the selectivity index on Vero normal cell line. Results are the average of triplicates.

Cpd. No.	IC ₅₀ (µM)	SI Vero	Cpd. No.	IC ₅₀ (µM)	SI * Vero
3	0.08 ± 0.62	0.087	12	0.04 ± 0.34	0.048
4	0.07 ± 0.36	0.094	13	0.08 ± 1.2	0.089
5	0.06 ± 0.35	0.34	14	0.05 ± 0.59	0.18
6	0.05 ± 0.44	0.083	15	0.02 ± 0.17	0.13
7	0.02 ± 0.11	0.99	16	0.08 ± 0.69	0.13
8	0.08 ± 0.32	0.14	17	0.02 ± 0.21	0.12
9	0.03 ± 0.29	0.10	18	0.05 ± 0.86	0.15
10	0.009 ± 0.09	0.13	19	0.02 ± 0.65	0.077
11	0.01 ± 0.11	0.13	20	0.01 ± 0.63	0.082

* SI (Selectivity index) = IC₅₀ on Vero cells/IC₅₀ on Caco-2.

2.2.2. Cell Cycle Progression

The potential candidates with anti-tumor effect on the Caco-2 cell line along with a high SI were chosen for cell-cycle analysis. The cell-cycle distribution and cell death were analyzed using Annexin V-FITC/PI staining and flow cytometry (Table 4, Figure 4). The potential candidates that showed potent anticancer activity against the Caco-2 cell line and high SI were chosen to investigate how they will change the cell-cycle distribution.

Table 4. Cell-cycle analysis of Caco-2 cells following treatment with the parent compounds and their derivatives.

Sample Data		Results		
Cpd. No.	%G0-G1	%S	%G2/M	%Pre-G1
Control (Caco-2)	53.61 ± 3.16	37.95 ± 2.25	8.44 ± 0.63	1.78 ± 0.08
1	46.29 ± 3.1	33.22 ± 1.99	20.49 ± 1.92	11.31 ± 0.81
2	39.77 ± 2.29	34.08 ± 2.63	26.15 ± 3.26	13.22 ± 0.63
5	41.52 ± 2.61	31.62 ± 1.79	26.86 ± 2.75	7.56 ± 0.39
7	28.68 ± 1.64	26.41 ± 2.15	44.91 ± 3.42	18.26 ± 1.42
9	38.51 ± 1.95	31.44 ± 2.87	30.05 ± 2.59	9.62 ± 0.37
10	29.75 ± 1.73	28.27 ± 1.99	41.98 ± 2.18	23.42 ± 2.12
11	41.09 ± 2.76	33.36 ± 2.73	25.55 ± 2.47	14.04 ± 0.95
14	34.28 ± 1.74	31.15 ± 3.17	34.57 ± 4.16	16.51 ± 0.63
15	26.59 ± 2.67	22.58 ± 2.91	50.83 ± 3.49	25.17 ± 3.29
17	42.11 ± 3.41	29.43 ± 3.16	28.46 ± 2.64	12.11 ± 0.97
18	33.26 ± 4.29	29.12 ± 4.05	37.62 ± 2.47	12.92 ± 2.16
20	39.12 ± 2.58	34.04 ± 2.69	26.84 ± 2.34	8.62 ± 0.69

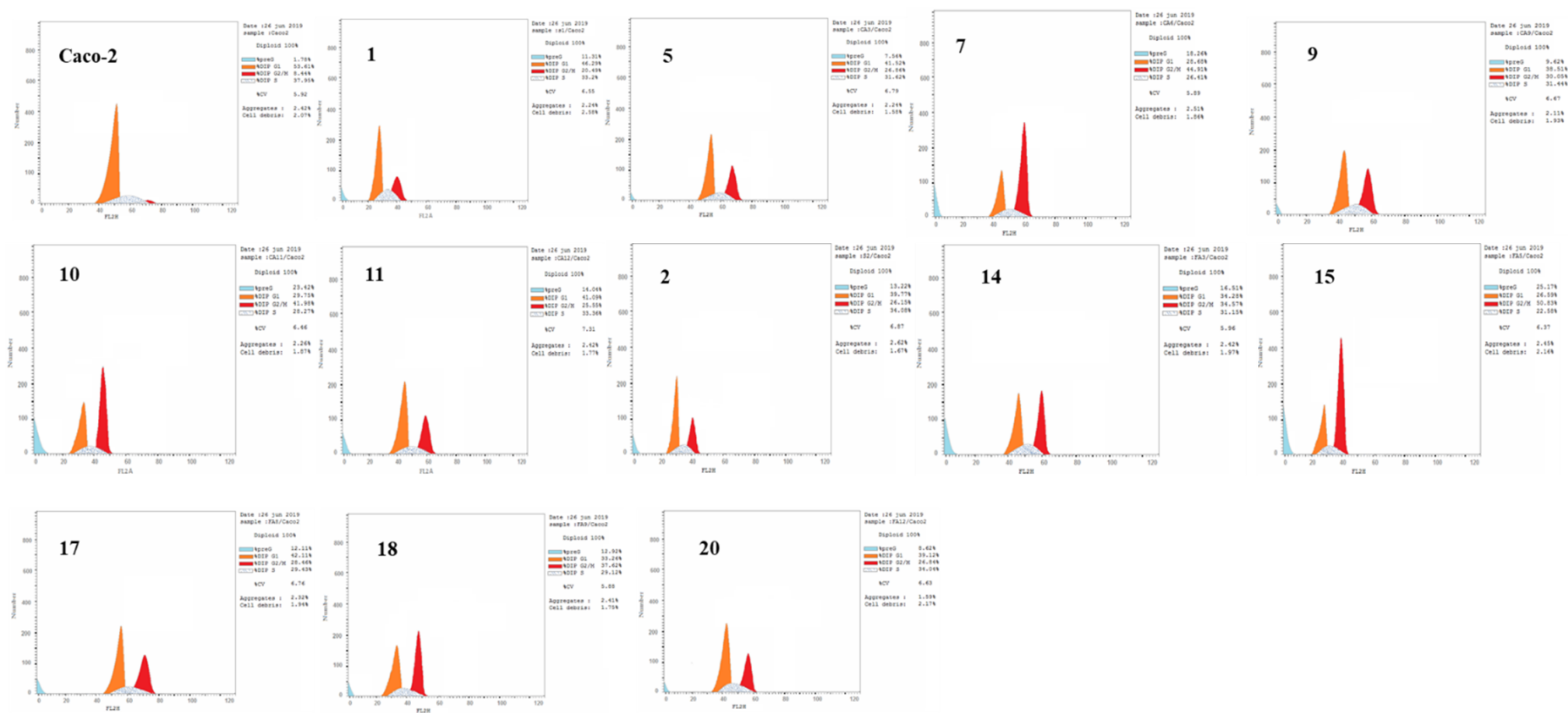


Figure 4. Cell-cycle analysis of Caco-2 cells following treatment with different derivatives and their parents; Histogram showing the percentages of cells in different cell cycle phases.

Flow Cytometry Analysis Showing Induction of Apoptosis

Cell-cycle analysis showed that the treatment of Caco-2 cells with the parent compounds and their derivatives resulted in an increase in the cell population in the G2/M phase, indicating apoptosis. In the case of caffeic acid derivatives, the highest induction of apoptosis was seen in compounds **10**, **7** and **11** (23.42%, 18.26% and 14.04%), respectively, which showed a more significant increase than the caffeic acid itself (11.31%). On the contrary, compounds **5** and **9** showed a non-significant increase in the apoptotic population compared to the parent compound **1** (Table 4).

Concerning Ferulic acid derivatives, the accumulation in the Pre-G1 phase and thus the highest induction of apoptosis was observed with candidates **15** and **14** (25.17% and 16.51% respectively) which showed a more significant effect than the parent compound **2** itself (13.22%), whereas the derivatives **17**, **18** and **20** showed non-significant decrease in the apoptotic population compared to parent compound **2**. (Table 4)

Evaluation of Apoptosis by Annexin V-FITC Staining

Quantification of the different types of apoptotic cells was of our interest due to the accumulation of cells at the G2/M phase during cell-cycle analysis following the treatment with the parent compounds **1** and **2** and their potential candidates.

After Caco-2 cells were treated with parent compounds **1** and **2** and their derivatives, they were stained with annexin V-FITC/PI, and then flow cytometry was used to detect the cell-cycle distribution as shown in Figure 5 and Table 5.

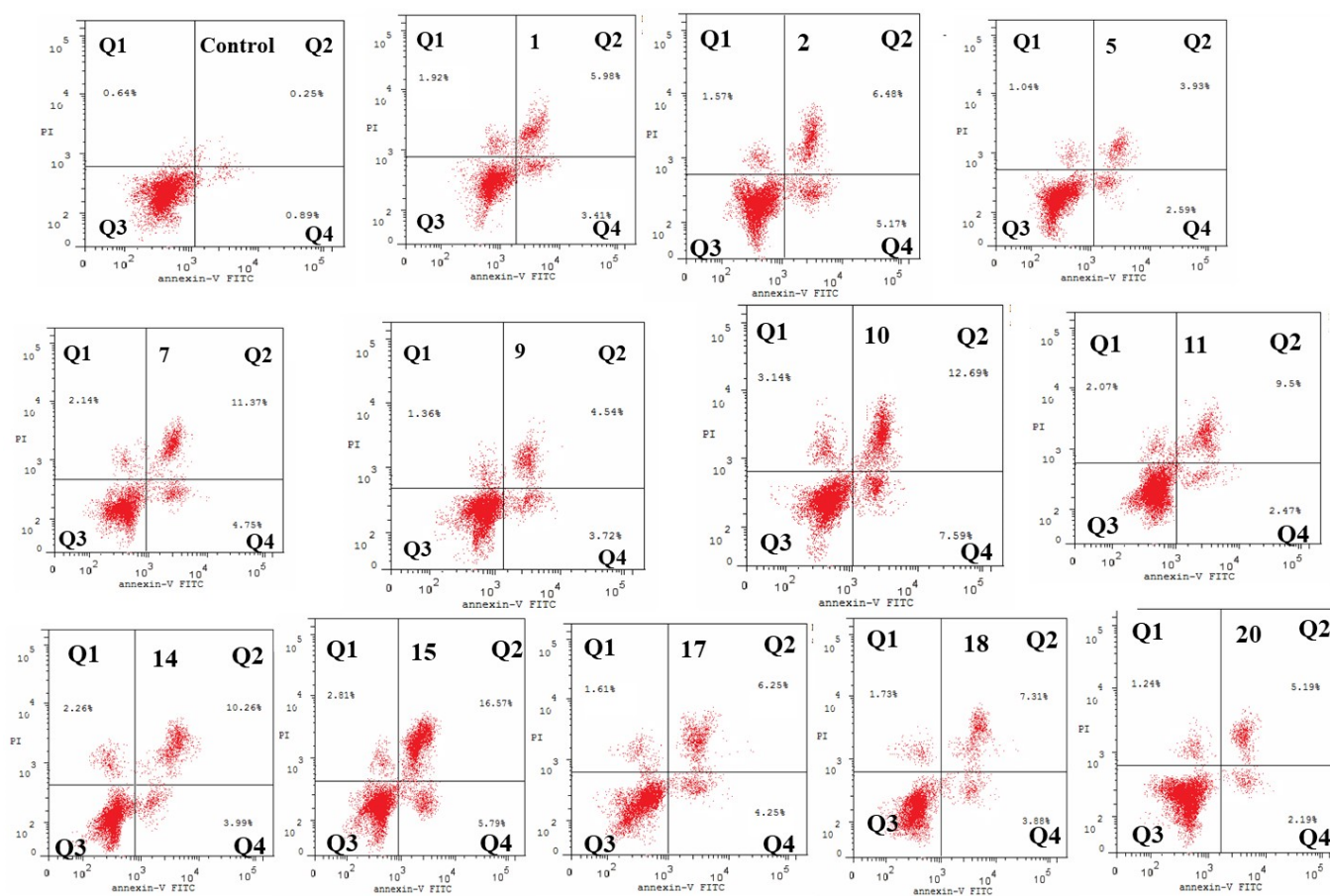


Figure 5. Dot plot representing four quadrant images observed by flow cytometry analysis. Q1: shows necrotic cells, Q2: shows later period apoptotic cells, Q3: shows normal cells and the Q4: shows early apoptotic cells.

Table 5. Detection of different types of apoptotic cells induced in Caco-2 cells following treatment with parent compounds and their derivatives using annexin-V FITC/PI staining.

Cpd. No.	Total	Early Apoptosis	Late Apoptosis	Necrosis
Control (Caco-2)	1.78	0.89	0.25	0.64
1	11.31	3.41	5.98	1.92
2	13.22	5.17	6.48	1.57
5	7.56	2.59	3.93	1.04
7	18.26	4.75	11.37	2.14
9	9.62	3.72	4.54	1.36
10	23.42	7.59	12.69	3.14
11	14.04	2.47	9.50	2.07
14	16.51	3.99	10.26	2.26
15	25.17	5.79	16.57	2.81
17	12.11	4.25	6.25	1.61
18	12.92	3.88	7.31	1.73
20	8.62	2.19	5.19	1.24

The results of the evaluation of apoptosis revealed that potential candidates **7**, **10**, **11**, **14** and **15** showed the highest proportion of cells in the late apoptotic stage (stained by Annexin V-FITC and PI).

2.2.3. Gene Expression

Caffeic Acid and Ferulic Acid Derivatives Enhanced Pro-Apoptotic Genes

The effect of caffeic acid **1** and its amide derivatives **5**, **7**, **9**, **10** and **11** as well as ferulic acid **2** and its derivatives **14**, **15**, **17**, **18**, and **20** on the expression of pro-apoptotic genes were tested. β -actin gene was used as a control gene. Gene expression was chosen over Western blotting for more accurate quantification and thus comparison. The gene expression of the p53, caspase 3 and Bax genes was measured. Most of the derivatives showed an increased expression of the three genes, which was evidenced by increasing apoptotic effects. In the case of caffeic acid derivatives, compound **10** showed the highest overexpression with an increase of 14- to 16-fold in the three genes, followed by **7** and **11** (Figure 6). Regarding the ferulic acid derivatives, **15** showed the highest overexpression of 10-fold in the p53 and 15-fold in the caspase 3 and Bax genes compared to the parent acid (Figure 7).

Caffeic Acid and Ferulic Acid Derivatives Inhibit Metastasis Enhancing Genes

Matrix metalloproteinases (MMPs) appear to play an important role in the formation and progression of human cancers. MMPs are involved in the breakdown of the extracellular matrix, which is a crucial stage in tumor invasion and spread [52]. A literature review revealed that both **1** and **2** decrease the expression of both MMP-2 and 9, which may lead to decrease in enzymatic activity [53].

To assess the effect of **1**, **2** and their derivatives **5**, **7**, **9**, **10**, **11**, **14**, **15**, **17**, **18**, and **20** on tumor progression and metastasis, the expression of the MMP2 and MMP9 was measured [54,55].

The derivatives of both **1** and **2** showed a significant decrease in the expression of both MMP2 and MMP9. Out of the most potential candidates, **17** and **7** showed the greatest inhibition in both groups (Figures 8 and 9).

2.3. Structure–Activity Relationship Correlation

The parent phenolic acids **1** and **2** were tested against five cancer cell lines: Caco-2, A549, PANC-1, MCF7, and Hep G2, as well as one normal Vero cell line using DOX as positive reference. The parent compounds showed significant antitumor activity against Caco-2 cell line and with excellent selectivity index (SI). Consequently, all the newly synthesized amide derivatives **3–20** were evaluated for their cytotoxic activity against Caco-2 cancer cell line. The SI of amide derivatives was determined using the Vero normal

cell line. They showed excellent cytotoxic activity, much more potent than the parent acids 1 and 2. Based on the phenolic acids scaffold, the amide derivatives were designed to have all the features of both acids as well as the stable amide linkage. All the amide derivatives 3–20 showed very promising anticancer activity against Caco-2 cell line and very good SI. So, changing the carboxylic acid moiety into an amide functionality increased the biological activity and did not destroy the selectivity index of the parent compounds. Examining the structure of the six most active compounds (7, 10, 11, 14, 15 and 17) (Figure 10), starting from the anticancer activity against Caco-2 cell line and excellent SI, followed by cell-cycle analysis and apoptosis assays, then the effect of these candidates on gene expression of p53, caspase 3, Bax, MMP-2 and MMP-9, it was found that besides all the features of both acids and the amide linkage, five compounds out of six have aromatic amide moieties. The presence of *p*-chloro on the phenyl ring of the amide linkage resulted in the most cytotoxic compound of all the six candidates. Replacing the chloro atom in compound 10 with bromo in compound 7 decreases the antitumor activity. Moreover, it was found that the presence of the cycloalkyl group of the amide linkage in the case of compound 15 increased the induction of apoptosis and showed the highest proportion of cells in late apoptotic stage. In case of enhancing the pro apoptotic genes (p53, caspase 3 and Bax), compound 10 (with *p*-chlorophenyl) revealed the highest activity. Furthermore, in case of inhibiting the metastasis-enhancing genes, compound 17 with *m*-tolyl group was the most active one.

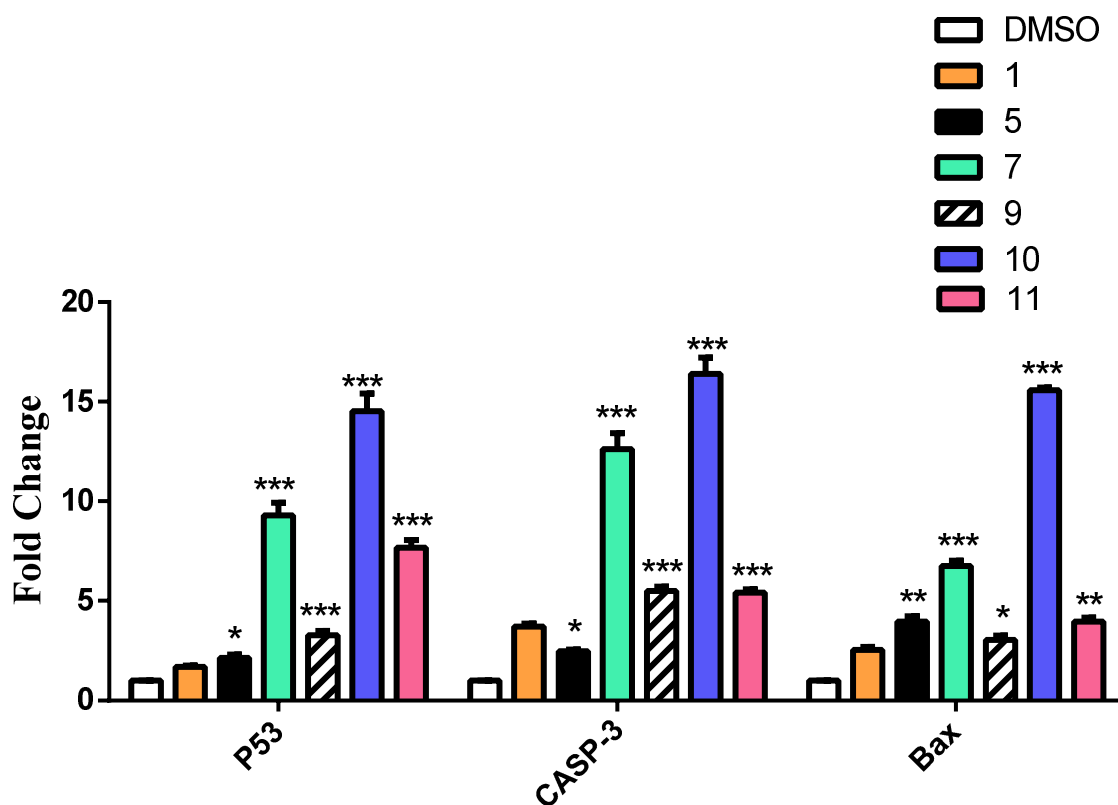


Figure 6. The effect of CA and its derivatives on the expression of P53, Caspase 3 and Bax genes by RT-qPCR. The results were represented as mean of fold changes \pm SD. β -actin gene was used as a control gene. * Significant from CA at $p < 0.05$, ** Significant from CA at $p < 0.01$, *** Significant from CA at $p < 0.001$.

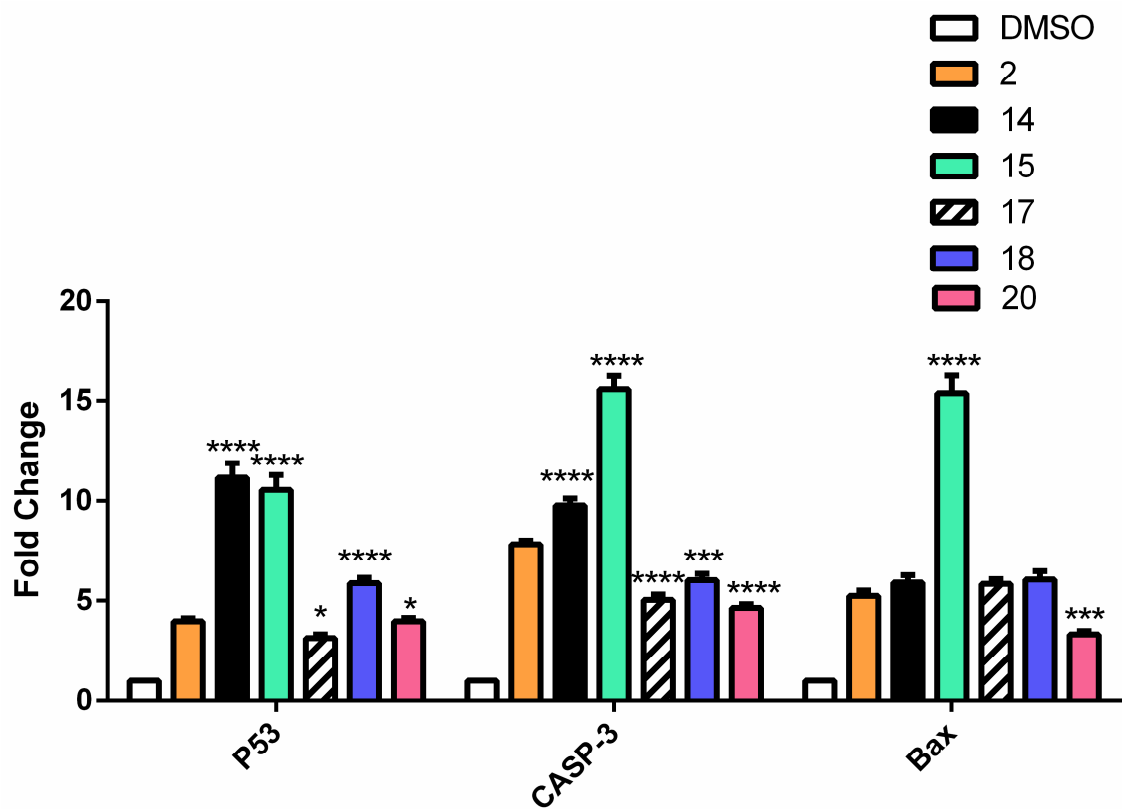


Figure 7. The effect of FA and its derivatives on the expression of P53, Caspase 3 and Bax genes by RT-qPCR. The results were represented as mean of fold changes \pm SD. β -actin gene was used as a control gene. * Significant from FA at $p < 0.05$, *** Significant from FA at $p < 0.001$, **** Significant from FA at $p < 0.0001$.

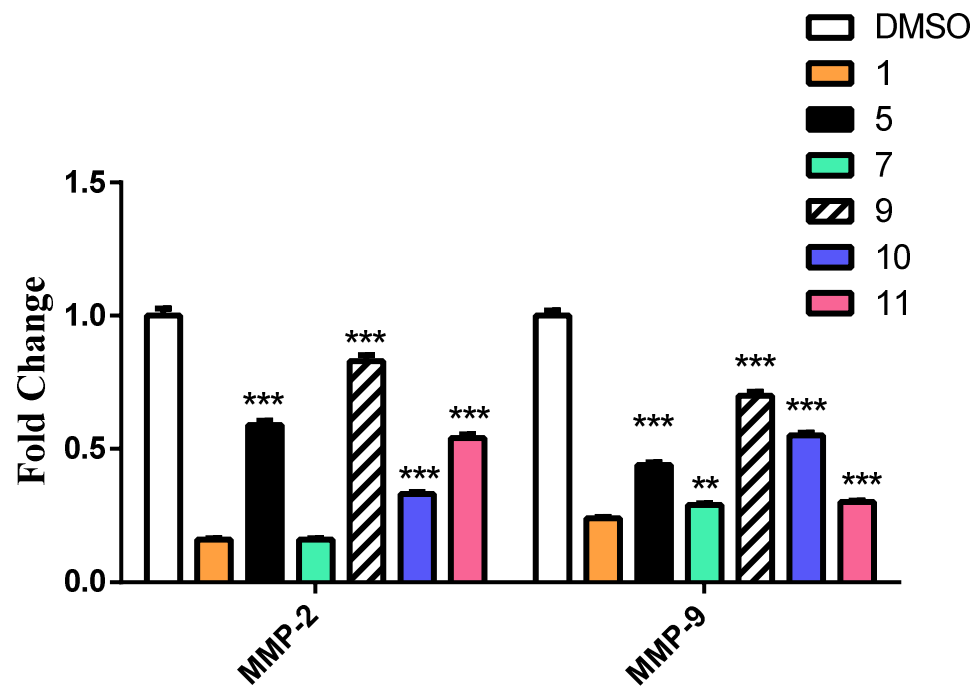


Figure 8. The effect of CA and its derivatives on the expression of MMP-2 and MMP-9 by RT-qPCR. The results were represented as mean of fold changes \pm SD. β -actin gene was used as a control gene. ** Significant from CA at $p < 0.01$, *** Significant from CA at $p < 0.001$.

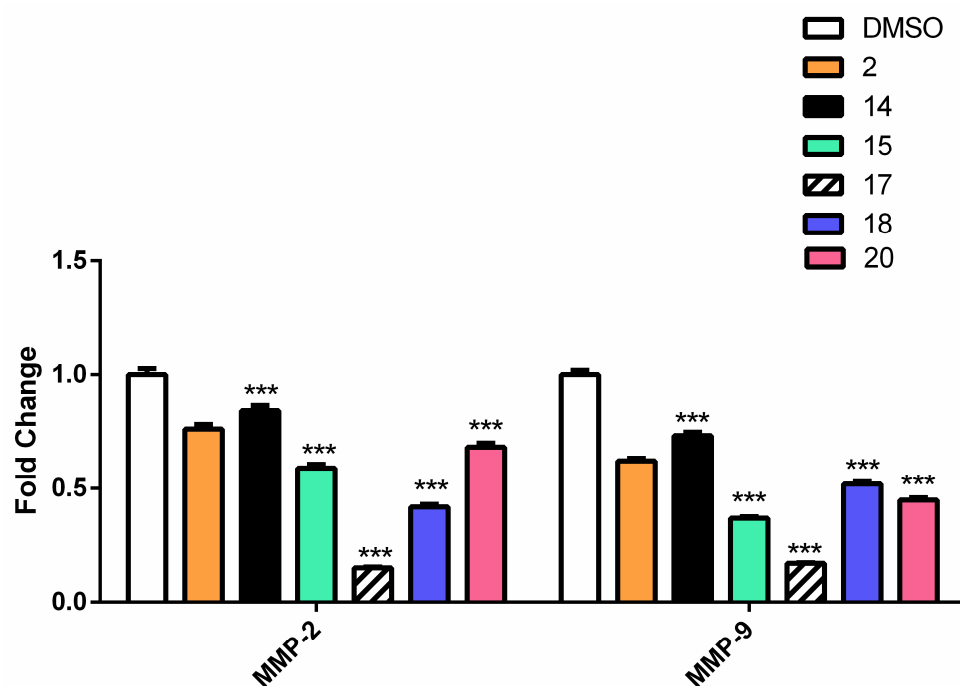


Figure 9. The effect of FA and its derivatives on the expression of MMP-2 and MMP-9 genes by RT-qPCR. The results were represented as mean of fold changes \pm SD. β -actin gene was used as a control gene. *** Significant from FA at $p < 0.001$.

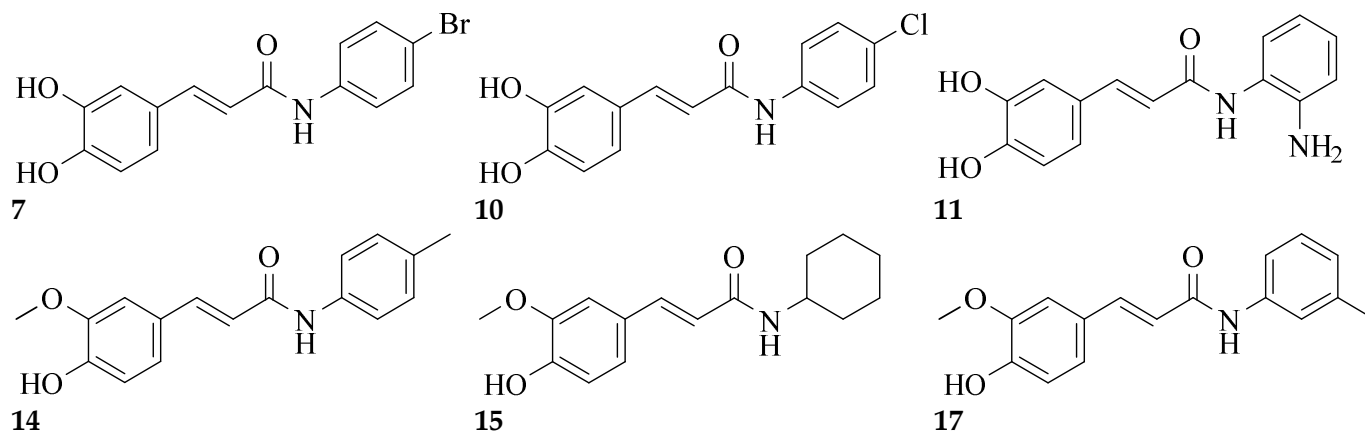


Figure 10. Structures of the most active compounds throughout all the biological tests.

3. Materials and Methods

3.1. General

Silica gel 60 (70–230 mesh ASTM; Fluka, Steinheim, Germany), Diaion HP-20 AG, Sephadex LH-20 (Pharmacia Fine Chemicals AB, Uppsala, Sweden) and silica gel GF₂₅₄ precoated thin layer plates (Fluka, Steinheim, Germany) were used. Chromatograms detections were performed under UV light (at 254 and 366 nm) and sprayed by *p*-anisaldehyde sulphuric acid spray reagent. Melting points ($^{\circ}$ C, uncorrected) were determined on Stuart apparatus and the given values were uncorrected. Progress of the reaction was monitored by thin layer chromatography (TLC) using aluminum sheets precoated with UV fluorescent silica gel (MERCK, Rahway, NJ, USA, 60 F 254), and spots were visualized by UV lamp. The solvent system used was dichloromethane: methanol (in different ratios). The IR spectra (cm^{-1}) were determined using KBr discs on a Shimadzu IR8400s Spectrophotometer (Microanalytical Unit, Faculty of Pharmacy, Cairo University, Cairo, Egypt). ^1H NMR and ^{13}C NMR spectra were performed on Bruker 400-BB 400 MHz Spectrophotometer, microanalytical unit, Faculty of Pharmacy, Cairo University, Cairo, Egypt, using tetramethylsilane

(TMS) as internal standard, and chemical shift values were recorded in ppm on δ scales. Peak multiplicities were designed as follows: s, singlet; d, doublet; t, triplet; m, multiplet. Elemental analyses were performed at the Regional Center for Mycology and Biotechnology, Faculty of Pharmacy, Al-Azhar University, Cairo, Egypt. The data were statistically evaluated using the Graph Pad Prism 6 program. Data were reported as mean \pm SD of the triplicates of each experiment. One-way ANOVA with multiple comparisons post-hoc tests were used for analysis. Results were considered significant at $p < 0.05$.

3.2. Plant Material

The grains of oats (*Avena sativa* L. Family Poaceae) were obtained from the Agricultural Research Center, Giza, Egypt. The plants were authenticated at Botany Department, Faculty of Science, Cairo University, Giza, Egypt. Voucher samples no (3-10-2018) of the plants were deposited at the Museum of the Pharmacognosy Department, Faculty of Pharmacy, Cairo University.

Extraction and Isolation of Caffeic and Ferulic Acids

The powdered oats (2 kg) were extracted with 80% ethanol at 55 °C for 165 min (14 L \times three times), the ethanolic extract was evaporated under vacuum at 40 °C. The ethanolic residue (350 gm) was suspended in distilled water (1 L) and defatted by methylene chloride (1 L \times 3 times), then the defatted aqueous solution was fractionated over a Dianion column using 100% water, methanol-water (1:1 *v/v*) and 100% methanol. The solvent in each case was evaporated under vacuum to obtain three fractions 100% water fraction (75 gm), MeOH-water (1:1) fraction (55 gm) and 100% methanol fraction 67 gm.

Part of the 100% methanol fraction (5 g) was purified was chromatographed over a sephadex LH-20 column (3 \times 30 cm), eluted with gradient elution 50%, 80% and 100% methanol (300 mL each). Fractions (10 mL, each) were collected and monitored by TLC (silica gel GF₂₅₄ precoated plates- Fluka) using solvent system (dichloromethane-methanol 9:1 *v/v*). Similar fractions were pooled together to obtain two pure compounds **1** (Rf 0.48, 500 mg, white crystals) and **2** (Rf 0.55, 750 mg, white crystals). This process was repeated several times to obtain 10 g of each compound.

3.3. Chemistry:

3.3.1. General method of Preparation of Caffeic or Ferulic Acid Amide Derivatives (3–20)

A mixture of either caffeic acid **1** or ferulic acid **2** (0.005 mol), the appropriate amine (0.005 mol) and DCC (1.03 g, 0.005 mol) in anhydrous THF (5 mL) was stirred in an ice-bath for an hour then left to stir at room temperature for 24 h. The mixture was filtered off then the filtrate was left to evaporate to dryness to provide compounds **3–20**. Purification of the final compounds was carried out using either crystallization or a glass column (2 \times 30 cm) of a sephadex LH-20 (Pharmacia Fine Chemicals AB, Uppsala, Sweden), through using (100% methanol) as eluent. Fractions 1 mL were collected and measured through using the TLC (silica gel GF₂₅₄ precoated plates-Fluka) using solvent system (n-hexane-ethyl acetate 8:2 *v/v*).

(E)-3-(3,4-Dihydroxyphenyl)-1-(4-phenylpiperazin-1-yl)prop-2-en-1-one (3)

IR (KBr, cm^{-1}): 3475 (OH), 3186 (C-H aromatic), 2944 (C-H aliphatic), 1639 (C=O). ¹H NMR (DMSO-*d*₆, D₂O, δ): 1.36–1.85 (m, 8H, 2 N-CH₂-CH₂), 6.76–7.26 [m, 10H (2OH, D₂O exchangeable + 8H Ar-H)], 7.35 and 7.39 (d, 2H, $J_{\text{value}} = 15.1\text{MHz}$, HC=CH); ¹³C NMR (100 MHz, DMSO-*d*₆, δ): 168.7, 149.8, 148.8, 141.8, 128.4, 127.6, 126.9, 125.9, 124.7, 116.9, 53.8, 49.6. Anal. Calcd. For C₁₉H₂₀N₂O₃ (324.37): C, 70.35; H, 6.21; N, 8.64. Found: C, 70.30; H, 6.30; N, 8.34.

(E)-3-(3,4-Dihydroxyphenyl)-N-(4-hydroxyphenyl)acrylamide (4)

IR (KBr, cm^{-1}): 3460, 3355, 3323, 3298 (OH and NH), 3130 (C-H aromatic), 1646 (C=O). ¹H NMR (DMSO-*d*₆, D₂O, δ): 6.40–6.49 (m, 4H, Ar), 6.59 and 6.84 (d, 2H, $J_{\text{value}} = 15\text{MHz}$,

CH=CH), 7.42 (s, 1H, NH), 7.46–7.50 (m, 3H, Ar), 9.86 (s, 3H, 3OH). ^{13}C NMR (100 MHz, DMSO- d_6 , δ): 170.2, 149.8, 147.9, 143.3, 138.5, 136.1, 127.1, 126.1, 129.1, 114.2, 112.6. Anal. Calcd. For $\text{C}_{15}\text{H}_{13}\text{NO}_4$ (271.26): C, 66.41; H, 4.83; N, 5.16. Found: C, 66.11; H, 4.53; N, 5.30.

(E)-3-(3,4-Dihydroxyphenyl)-N-(p-tolyl)acrylamide (5)

IR (KBr, cm^{-1}): 3510, 3420, 3348 (OH and NH), 3140 (C-H aromatic), 2910 (C-H aliphatic), 1652 (C=O). ^1H NMR (DMSO- d_6 , D_2O , δ): 2.26 (s, 3H, CH_3), 6.66–6.46 (m, 4H, Ar), 6.81 and 7.13 (d, 2H, $J_{\text{value}} = 14.9$ MHz, CH=CH), 7.50 (s, 1H, NH), 7.60–7.43 (m, 3H, Ar), 10.0 (s, 2H, 2OH). ^{13}C NMR (100 MHz, DMSO- d_6 , δ): 165.5, 149.5, 147.2, 143.3, 138.1, 137.5, 129.4, 128.6, 127.1, 125.3, 124.7, 114.7, 111.9, 21.7. Anal. Calcd. For $\text{C}_{16}\text{H}_{15}\text{NO}_3$ (269.29): C, 71.36; H, 5.61; N, 5.20. Found: C, 71.66; H, 5.81; N, 5.44.

(E)-N-Cyclohexyl-3-(3,4-dihydroxyphenyl)acrylamide (6)

IR (KBr, cm^{-1}): 3467, 3345, 3360 (OH and NH), 2956 (C-H aliphatic), 1667 (C=O). ^1H NMR (DMSO- d_6 , D_2O , δ): 1.00–1.76 (m, 10H, CH_2), 3.42 (m, 1H, CH), 5.70 and 5.72 (d, 2H, $J_{\text{value}} = 15$ MHz HC=CH), 6.76–7.26 (m, 3H, Ar-H + 2OH, NH, D_2O exchangeable). ^{13}C NMR (100 MHz, DMSO- d_6 , δ): 166.8, 148.9, 147.5, 143.9, 138.9, 129.4, 127.3, 125.1, 123.3, 122.7, 116.7, 110.9, 51.7, 31.5, 25.9; Anal. Calcd. For $\text{C}_{15}\text{H}_{19}\text{NO}_3$ (261.31): C, 68.94; H, 7.33; N, 5.36. Found: C, 68.74; H, 7.53; N, 5.16.

(E)-N-(4-Bromophenyl)-3-(3,4-dihydroxyphenyl)acrylamide (7)

IR (KBr, cm^{-1}): 3413, 3327, 3317 (OH and NH), 3200 (C-H aromatic), 1662 (C=O). ^1H NMR (DMSO- d_6 , D_2O , δ): 6.50–7.51 (m, 9H, 2OH D_2O exchangeable + Ar-H), 7.58 and 7.66 (d, 2H, $J_{\text{value}} = 15.0$ MHz HC=CH), 10.17 (s, 1H, NH) ppm. ^{13}C NMR (100 MHz, DMSO- d_6 , δ): 170.9, 148.9, 146.3, 145.3, 136.3, 131.5, 128.9, 127.9, 126.8, 126.1, 121.7, 115.1, 111.9. Anal. Calcd. For $\text{C}_{15}\text{H}_{12}\text{BrNO}_3$, (334.16): C, 53.91; H, 3.62; Br, 23.91; N, 4.19. Found: C, 53.71; H, 3.69; N, 4.30.

(E)-N-(4-Methoxyphenyl)-3-(3,4-dihydroxyphenyl)acrylamide (8)

IR (KBr, cm^{-1}): 3510, 3468, 3420 (OH and NH), 3130 (C-H aromatic), 1646 (C=O). ^1H NMR (DMSO- d_6 , D_2O , δ): 3.63 (s, 3H, OCH_3), 6.50–7.40 (m, 7H, Ar-H), 7.60 and 7.62 (d, 2H, $J_{\text{value}} = 14.8$ MHz, HC=CH), 9.1–9.44 (s, 2H, 2OH, D_2O exchangeable), 9.94 (s, 1H, NH D_2O exchangeable) ppm. ^{13}C NMR (100 MHz, DMSO- d_6 , δ): 165.9, 148.9, 146.3, 143.3, 139.3, 135.5, 129.9, 127.9, 126.8, 125.1, 121.7, 114.1, 113.9, 56.9. Anal. Calcd. For $\text{C}_{16}\text{H}_{15}\text{NO}_4$ (285.29): C, 67.36; H, 5.30; N, 4.91. Found: C, 67.56; H, 5.39; N, 4.71.

(E)-N-Benzyl-3-(3,4-dihydroxyphenyl)acrylamide (9)

IR (KBr, cm^{-1}): 3300–3350 (OH and NH), 3135 (C-H aromatic), 2927 (C-H aliphatic), 1626 (C=O). ^1H NMR (DMSO- d_6 , D_2O , δ): 5.59 (CH_2), 6.52 and 6.56 (d, 2H, $J_{\text{value}} = 15.3$ MHz, HC=CH), 6.77–7.51 (m, 8H, Ar-H), 9.21 and 9.45 (2H, OH, D_2O exchangeable), 9.98 (s, 1H, NH, D_2O exchangeable), ^{13}C NMR (100 MHz, DMSO- d_6 , δ): 167.9, 146.9, 145.3, 141.3, 137.3, 128.9, 127.2, 126.8, 126.4, 123.7, 115.1, 112.9, 43.9. Anal. Calcd. For $\text{C}_{16}\text{H}_{15}\text{NO}_3$ (269.29): C, 71.36; H, 5.61; N, 5.20. Found: C, 79.36; H, 5.81; N, 5.34.

(E)-N-(4-Chlorophenyl)-3-(3,4-dihydroxyphenyl)acrylamide (10)

IR (KBr, cm^{-1}): 3510, 3413, 3317 (OH and NH), 3200 (C-H aromatic), 1635 (C=O). ^1H NMR (DMSO- d_6 , D_2O , δ): 6.50–7.02 [m, 9H (2OH, D_2O exchangeable + 7H, Ar-H)], 7.71 and 7.73 (d, 2H, $J_{\text{value}} = 14.8$ MHz, HC=CH), 10.209 (s, 1H, NH) ppm, ^{13}C NMR (100 MHz, DMSO- d_6 , δ): 169.9, 148.5, 146.9, 144.3, 143.3, 133.3, 128.9, 127.2, 126.1, 124.7, 123.7, 117.9, 117.1, 113.9. Anal. Calcd. For $\text{C}_{15}\text{H}_{12}\text{ClNO}_3$ (289.71): C, 62.19; H, 4.17; N, 4.83. Found: C, 62.28; H, 4.30; N, 4.89.

(E)-N-(2-Aminophenyl)-3-(3,4-dihydroxyphenyl)acrylamide (11)

IR (KBr, cm^{-1}): 3500–3240 (OH, NH and NH_2), 3200 (C-H aromatic), 1662 (C=O). ^1H NMR (DMSO-d_6 , D_2O , δ): 5.59 (CH_2), 6.52 and 6.56 (d, 2H, $J_{\text{value}} = 15.3$ MHz, $\text{HC}=\text{CH}$), 6.27–7.52 (m, 8 H, Ar-H), 9.17 (s, 2H, NH_2 , D_2O exchangeable), 9.27 (s, 1H, NH, D_2O exchangeable), 9.43 and 9.48 (2H, OH, D_2O exchangeable). ^{13}C NMR (100 MHz, DMSO-d_6 , δ): 168.7, 149.5, 146.9, 145.3, 141.3, 128.4, 127.6, 125.3, 124.5, 122.7, 117.2, 118.9, 114.9. Anal. Calcd. For $\text{C}_{15}\text{H}_{14}\text{N}_2\text{O}_3$ (270.28): C, 66.66; H, 5.22; N, 10.36. Found: C, 66.37; H, 5.02; N, 10.44.

(E)-3-(3-Hydroxy-4-methoxyphenyl)-1-(4-phenylpiperazin-1-yl)prop-2-en-1-one (12)

IR (KBr, cm^{-1}): 3435 (OH), 3140 (C-H aromatic), 2910 (C-H aliphatic), 1629 (C=O). ^1H NMR (DMSO-d_6 , D_2O , δ): 1.04–1.81 (m, 8H, 2 N- $\text{CH}_2\text{-CH}_2$), 3.36 (s, 3H, OCH_3), 6.78–6.74 (m, 3H, Ar), 6.90 and 6.98 (d, 2H, $J_{\text{value}} = 15.2$ MHz, $\text{CH}=\text{CH}$), 7.24–7.18 (m, 5H, Ar), 8.08 (s, 1H, OH). ^{13}C NMR (100 MHz, DMSO-d_6 , δ): 160.7, 149.5, 148.9, 141.3, 128.4, 127.6, 126.1, 125.3, 124.7, 118.9, 55.7, 53.1, 48.6. Anal. Calcd. For $\text{C}_{20}\text{H}_{22}\text{N}_2\text{O}_3$ (338.40): C, 70.99; H, 6.55; N, 8.28. Found: C, 70.73; H, 6.61; N, 8.31.

(E)-3-(3-Hydroxy-4-methoxyphenyl)-N-(4-methoxyphenyl)acrylamide (13)

IR (KBr, cm^{-1}): 3379, 3116 (OH and NH), 3066 (C-H aromatic), 2924 (C-H aliphatic), 1651 (C=O). ^1H NMR (DMSO-d_6 , D_2O , δ): 3.83 (s, 3H, OCH_3), 6.40–6.49 (m, 4H, Ar), 6.59 and 6.84 (d, 2H, $J_{\text{value}} = 15.1$ MHz, $\text{CH}=\text{CH}$), 7.42 (s, 1H, NH), 7.46–7.50 (m, 3H, Ar), 9.86 (s, 2H, OH). ^{13}C NMR (100 MHz, DMSO-d_6 , δ): 169.7, 149.5, 148.9, 142.3, 138.1, 136.5, 126.1, 125.3, 129.7, 114.5, 112.9, 55.7, 53.7. Anal. Calcd. For $\text{C}_{16}\text{H}_{15}\text{NO}_4$ (285.29): C, 67.36; H, 5.30; N, 4.91. Found: C, 67.21; H, 5.43; N, 4.82.

(E)-3-(3-Hydroxy-4-methoxyphenyl)-N-(p-tolyl)acrylamide (14)

IR (KBr, cm^{-1}): 3460, 3290 (OH and NH), 3089 (C-H aromatic), 2846 (C-H aliphatic), 1645 (C=O). ^1H NMR (DMSO-d_6 , D_2O , δ): 2.26 (s, 3H, CH_3), 3.83 (s, 3H, OCH_3), 6.46–6.66 (m, 4H, Ar), 6.81 and 7.13 (d, 2H, $J_{\text{value}} = 15.2$ MHz, $\text{CH}=\text{CH}$), 7.50 (s, 1H, NH), 7.60–7.43 (m, 3H, Ar), 10.0 (s, 1H, OH). ^{13}C NMR (100 MHz, DMSO-d_6 , δ): 165.8, 149.5, 147.9, 144.3, 138.1, 136.5, 129.4, 128.6, 126.1, 125.3, 124.7, 112.7, 111.9, 55.9, 22.7. Anal. Calcd. For $\text{C}_{17}\text{H}_{17}\text{NO}_3$ (283.32): C, 72.07; H, 6.05; N, 4.94. Found: C, 72.37; H, 6.25; N, 4.74.

(E)-N-Cyclohexyl-3-(4-hydroxy-3-methoxyphenyl)acrylamide (15)

IR (KBr, cm^{-1}): 3380, 3240 (OH and NH), 2920 (C-H aliphatic), 1655 (C=O). ^1H NMR (DMSO-d_6 , D_2O , δ): 1.05–1.71 (m, 10H, CH_2), 3.37 (m, 1H, CH), 3.84 (s, 3H, OCH_3), 5.70 and 5.72 (d, 2H, $J_{\text{value}} = 15.9$ MHz, $\text{HC}=\text{CH}$), 6.76–7.26 (m, 3H, Ar-H + 1OH, 1NH, D_2O exchangeable), ^{13}C NMR (100 MHz, DMSO-d_6 , δ): 169.8, 148.9, 147.1, 143.3, 138.1, 129.4, 127.6, 125.1, 123.3, 122.7, 116.7, 110.9, 56.2, 50.7, 32.5, 24.9; Anal. Calcd. For $\text{C}_{16}\text{H}_{21}\text{NO}_3$ (275.34): C, 69.79; H, 7.69; N, 5.09. Found: C, 69.97; H, 7.79; N, 5.00.

(E)-3-(4-Hydroxy-3-methoxyphenyl)-N-(4-methoxyphenyl)acrylamide (16)

IR (KBr, cm^{-1}): 3460, 3344 (OH and NH), 3050 (C-H aromatic), 2908, 2839 (C-H aliphatic), 1635 (C=O). ^1H NMR (DMSO-d_6 , D_2O , δ): 3.81 (s, 3H, OCH_3), 3.84 (s, 3H, OCH_3), 6.68 and 7.05 (d, 2H, $J_{\text{value}} = 15.4$ MHz, $\text{CH}=\text{CH}$), 6.88–6.83 (m, 4H, Ar), 7.54–7.47 (m, 3H, Ar-H), 7.54 (s, 1H, NH), 10.01 (s, 1H, OH). ^{13}C NMR (100 MHz, DMSO-d_6 , δ): 165.8, 148.5, 147.9, 144.3, 138.1, 130.3, 129.4, 127.6, 126.1, 124.3, 122.7, 114.7, 112.9, 56.2, 55.7; Anal. Calcd. For $\text{C}_{17}\text{H}_{17}\text{NO}_4$ (299.32): C, 68.21; H, 5.72; N, 4.68. Found: C, 68.25; H, 5.63; N, 4.55.

(E)-3-(3-Hydroxy-4-methoxyphenyl)-N-(m-tolyl)acrylamide (17)

IR (KBr, cm^{-1}): 3460, 3344 (OH and NH), 3050 (C-H aromatic), 2908 (C-H aliphatic), 1630 (C=O). ^1H NMR (DMSO-d_6 , D_2O , δ): 2.29 (s, 3H, CH_3), 3.84 (s, 3H, OCH_3), 6.68 and 7.06 (d, 2H, $J_{\text{value}} = 15.0$ MHz, $\text{CH}=\text{CH}$), 6.88–6.83 (m, 4H, Ar-H), 7.54–7.47 (m, 3H, Ar), 7.54 (s, 1H, NH), 10.01 (s, 1H, OH). ^{13}C NMR (100 MHz, DMSO-d_6 , δ): 165.6, 149.3, 147.1,

143.3, 139.6, 128.4, 126.6, 126.1, 122.3, 121.7, 114.4, 113.7, 56.9; Anal. Calcd. For C₁₇H₁₇NO₃ (283.32): C, 72.07; H, 6.05; N, 4.94. Found: C, 71.95; H, 6.32; N, 4.79.

(E)-N-Benzyl-3-(3-hydroxy-4-methoxyphenyl)acrylamide (18)

IR (KBr, cm⁻¹): 3425, 3380 (OH and NH), 3120 (C-H aromatic), 2839 (C-H aliphatic), 1640 (C=O). ¹H NMR (DMSO-d₆, D₂O, δ): 3.19 (s, 2H, CH₂), 3.81 (s, 3H, OCH₃), 6.57 and 6.83 (d, 2H, *J*_{value} = 15.2 MHz, CH=CH), 7.15 (s, 1H, NH), 7.74–7.23 (m, 8H, Ar-H), 9.86 (s, 1H, OH). ¹³C NMR (100 MHz, DMSO-d₆, δ): 167.6, 149.1, 147.9, 141.3, 137.6, 128.4, 126.6, 126.1, 122.3, 120.7, 114.4, 112.7, 56.4, 43.6; Anal. Calcd. For C₁₇H₁₇NO₃ (283.32): C, 72.07; H, 6.05; N, 4.94. Found: C, 72.07; H, 6.05; N, 4.94.

(E)-N-(4-Chlorophenyl)-3-(4-hydroxy-3-methoxyphenyl)acrylamide (19)

IR (KBr, cm⁻¹): 3460, 3290 (OH and NH), 3089 (C-H aromatic), 2846 (C-H aliphatic), 1630 (C=O). ¹H NMR (DMSO-d₆, D₂O, δ): 3.83 (s, 3H, OCH₃), 6.66–6.46 (m, 3H, Ar-H), 7.05 and 7.37 (d, 2H, *J*_{value} = 14.7 MHz, CH=CH), 7.20 (s, 1H, NH), 7.15–7.40 (m, 4H, Ar), 9.55 (s, 1H, OH). ¹³C NMR (100 MHz, DMSO-d₆, δ): 165.6, 149.1, 147.9, 141.3, 135.6, 133.5, 131.6, 129.7, 122.4, 121.9, 118.3, 116.7, 111.3, 56.1; Anal. Calcd. For C₁₆H₁₄ClNO₃ (303.74): C, 63.27; H, 4.65; N, 4.61. Found: C, 63.27; H, 4.65; N, 4.61.

(E)-N-(2-Aminophenyl)-3-(3-hydroxy-4-methoxyphenyl)acrylamide (20)

IR (KBr, cm⁻¹): 3447, 3345 (OH, NH and NH₂), 3022 (C-H aromatic), 2974 (C-H aliphatic), 1642 C=O. ¹H NMR (DMSO-d₆, D₂O, δ): 3.83 (s, 3H, OCH₃), 4.94 (s, 1H, NH₂), 6.61–6.37 (m, 4H, Ar-H), 6.75 and 6.85 (d, 2H, *J*_{value} = 14.9 MHz, CH=CH), 7.20 (s, 1H, NH), 7.50–7.35 (m, 3H, Ar-H), 9.28 (s, 1H, OH), ¹³C NMR (100 MHz, DMSO-d₆, δ): 168.00, 149.1, 147.9, 147.2, 141.3, 127.7, 125.9, 125.3, 122.9, 118.3, 114.7, 112.3, 56.8; Anal. Calcd. For C₁₆H₁₆N₂O₃ (284.30): C, 67.59; H, 5.67; N, 9.85. Found: C, 67.77; H, 5.51; N, 9.73.

3.4. Biological Activity

3.4.1. Cell Culture

MCF-7 cells (Human breast adenocarcinoma), HepG2 (human hepatocellular carcinoma), A549 (human lung adenocarcinoma), Caco-2 (colon carcinoma), PANC-1 (human pancreatic cancer), and Vero cells (derived from normal kidney cells) were supplied by (Holding Company for Biological Products and Vaccines VACSERA; Giza, Egypt). The cells were cultured in PRMI 1640 medium (Lonza, Switzerland) supplemented with 10% fetal bovine serum (Gibco), 1% penicillin and 1% streptomycin (Sigma Aldrich, Saint Louis, MO, USA) at 37 °C under an atmosphere of 5% CO₂ and 95% air.

3.4.2. Cell Viability Determination by MTT Assay

The effect of parent compounds and their derivatives were assessed by (3-(4,5-dimethylthiazol-2-yl)-2,5-diphenyl-tetrazolium bromide) MTT assay. On a 96-well tissue culture plate, all cell lines were inoculated at a density of 1 × 10⁵ cells/mL (100 µL/well) and incubated at 37 °C for 24 h in order to form a complete monolayer sheet. After a merged sheet of cells developed, the growth media was decanted from the 96-well microtiter and refilled with different concentrations of compounds (µg/mL), and the plate was incubated at 37 °C for 48 h to minimize exposure to the dissolving agent [56] (Supporting information).

MTT solution (BIO BASIC CANADA INC) was prepared [5 mg/mL in phosphate buffered saline (PBS)], added to each well and incubated for 4 h, then after removing the media, 200 µL of DMSO was added to each well to solubilize the formazan crystals and the optical density of the formazan product was measured at 560 nm using microplate reader (mindray, MR-96A). The results were calculated as the mean of the three independent experiments.

3.4.3. Annexin V/Propidium Iodide (PI) Apoptosis Assay by Flow Cytometry

In order to determine the percentage of viable, apoptotic and necrotic cells after treatment with our compounds, double-staining with fluorescein isothiocyanate (FITC) and PI was performed. Annexin V-FITC Apoptosis Detection Kit (BioVision, CA, USA) was used. Briefly, cultured Caco-2 were treated with the tested compounds or DMSO for 24h. Cells were then collected by centrifugation at 2000 rpm for 5 min, and the pellet was washed with PBS then centrifuged again at 2000 rpm for 5 min then resuspended in 500 μ L of the kit's binding buffer before adding the Annexin V-FITC and PI. The cells were then incubated at room temperature in the dark for 5 min. Annexin V-FITC binding was measured using FACS Calibur flow cytometer (BD biosciences, USA) (Ex = 488 nm, Em = 533 nm, FL1 filter for annexin and FL2 filter for PI).

3.4.4. Quantitative Polymerase Chain Reaction (qPCR) and RNA Extraction

The treated cells were harvested and the total RNA was extracted using RNeasy Mini Kit (Qiagen) according to the manufacturer's instruction. The primers of the required genes (Table 6) were used for SYBR Green qRT-PCR using a one-step RT-PCR kit with SYBR Green (Bio-Rad). qRT-PCR was performed on Rotor Gene Q (Qiagen). The mRNA levels of p53, Bcl-2, Caspase-3, Bax, MMP-2, and MMP-9 were calculated using the $2^{-\Delta\Delta CT}$ method with the endogenous β -actin mRNA as control to normalize the values. Rotor-Gene 6000 Series Software was used for data analysis. and their HGNC ID was added (Table 6)

Table 6. Primers used in qRT-PCR.

Gene	Primers Used
p53	F 5'-CCCCTCCTGGCCCCTGTCATCTTC-3' R 5'-GCAGCGCCTCACAACCTCCGTCAT-3'
Bcl-2	F 5'-CCTGTGGATGACTGAGTACC-3' R 5'-GAGACAGCCAGGAGAAATCA-3'
Caspase 3	F 5'-TTCATTATTCAGGCCCTGCCGAGG-3' R 5'-TTCTGACAGGCCATGTCATCCTCA-3'
Bax	F 5'-GTTTCATCCAGGATCGAGCAG-3' R 5'-CATCTTCTCCAGATGGTGA-3'
MMP-2	F 5'-CAAAAACAAGAAGACATACATCTT-3' R 5'-CAAAAACAAGAAGACATACATCTT-3'
MMP-9	F 5'-TGGGGGGCAACTCGGC-3' R 5'-GGAATGATCTAAGCCCAG-3'
β -actin	F 5'-GTGACATCCACACCCAGAGG-3' R 5'-ACAGGATGTCAAAACTGCC-3'

4. Conclusions

Despite the high efficacy of CA and FA, they are limited by their high metabolism and consequent low bioavailability. Therefore, we were challenged to synthesize highly stable and biologically active compounds. Henceforth, we designed and investigated 18 congeners of amide nature; they were all superior to their parent acids in terms of cytotoxic activity against Caco-2. The selected candidates for cell-cycle analysis and gene expression assays were those displaying superior cytotoxicity and high SI using Vero normal cells.

Subsequently, the assays offered six remarkably active compounds, **7**, **10**, **11**, **14**, **15** and **17**, and five of them comprised an aromatic ring adjacent to the amide bridge. In accordance with the SAR, the highest cytotoxicity was evident amongst the aromatic derivative with *p*-chloro phenyl **10**, displaying excellent cytotoxic activity, this was deduced when the cytotoxicity decreased after the chloro residue was replaced with a bromo substitution. It could also be concluded that overall, the caffeic acid amides surpassed the ferulic analogues.

We are planning to further study other amide derivatives and assess their activity in a suitable animal model.

Supplementary Materials: The following supporting information can be downloaded at: <https://www.mdpi.com/article/10.3390/molecules27196724/s1>, The charts of ¹HNMR of all the synthesized compounds.

Author Contributions: S.M.E.: Conceptualization, Supervision, Methodology, Reviewing and Editing. H.E.S.T.: Investigation, Methodology, Data analysis, Original draft preparation. I.G.S.: Investigation, Methodology, Data analysis, Original draft preparation. A.M.H.: Investigation, Methodology, Original draft preparation. A.M.K.: Conceptualization, Supervision, Methodology, Reviewing and Editing. N.M.A.: Investigation, Methodology, Data analysis, Original draft preparation. All authors have read and agreed to the published version of the manuscript.

Funding: This research received no external funding.

Institutional Review Board Statement: Not applicable.

Informed Consent Statement: Not applicable.

Data Availability Statement: Not applicable.

Conflicts of Interest: The authors declare no conflict of interest.

Sample Availability: Samples of the compounds are not available from the authors.

References

1. Mattiuzzi, C.; Lippi, G. Current Cancer Epidemiology. *J. Epidemiol. Glob. Health* **2019**, *9*, 217–222. [CrossRef] [PubMed]
2. Verma, A.; Laakso, I.; Seppänen-Laakso, T.; Huhtikangas, A.; Riekkola, M.L. A simplified procedure for indole alkaloid extraction from *Catharanthus roseus* combined with a semi-synthetic production process for vinblastine. *Molecules* **2007**, *12*, 1307–1315. [CrossRef] [PubMed]
3. Lichota, A.; Gwozdziński, K. Anticancer Activity of Natural Compounds from Plant and Marine Environment. *Int. J. Mol. Sci.* **2018**, *19*, 3533. [CrossRef] [PubMed]
4. Canel, C.; Moraes, R.M.; Dayan, F.E.; Ferreira, D. Podophyllotoxin. *Phytochemistry* **2000**, *54*, 115–120. [CrossRef]
5. Gomes, C.A.; da Cruz, T.G.; Andrade, J.L.; Milhazes, N.; Borges, F.; Marques, M.P.M. Anticancer activity of phenolic acids of natural or synthetic origin: A structure–activity study. *J. Med. Chem.* **2003**, *46*, 5395–5401. [CrossRef]
6. Dai, J.; Mumper, R.J. Plant phenolics: Extraction, analysis and their antioxidant and anticancer properties. *Molecules* **2010**, *15*, 7313–7352. [CrossRef]
7. Panwar, R.; Sharma, A.K.; Kaloti, M.; Dutt, D.; Pruthi, V. Characterization and anticancer potential of ferulic acid-loaded chitosan nanoparticles against ME-180 human cervical cancer cell lines. *Appl. Nanosci.* **2016**, *6*, 803–813. [CrossRef]
8. Elansary, H.O.; Szopa, A.; Kubica, P.; Al-Mana, F.A.; Mahmoud, E.A.; El-Abedin, T.K.A.Z.; Mattar, M.A.; Ekiert, H. Phenolic compounds of *Catalpa speciosa*, *Taxus cuspidata*, and *Magnolia acuminata* have antioxidant and anticancer activity. *Molecules* **2019**, *24*, 412. [CrossRef]
9. Genaro-Mattos, T.C.; Maurício, Â.Q.; Rettori, D.; Alonso, A.; Hermes-Lima, M. Antioxidant activity of caffeic acid against iron-induced free radical generation—A chemical approach. *PLoS ONE* **2015**, *10*, e0129963.
10. Kilani-Jaziri, S.; Mokdad-Bzeouich, I.; Krifa, M.; Nasr, N.; Ghedira, K.; Chekir-Ghedira, L. Immunomodulatory and cellular anti-oxidant activities of caffeic, ferulic, and p-coumaric phenolic acids: A structure–activity relationship study. *Drug Chem. Toxicol.* **2017**, *40*, 416–424. [CrossRef]
11. Kadar, N.N.M.A.; Ahmad, F.; Teoh, S.L.; Yahaya, M.F. Caffeic Acid on Metabolic Syndrome: A Review. *Molecules* **2021**, *26*, 5490. [CrossRef] [PubMed]
12. Maity, S.; Kinra, M.; Nampoothiri, M.; Arora, D.; Pai, K.S.R.; Mudgal, J. Caffeic acid, a dietary polyphenol, as a promising candidate for combination therapy. *Chem. Pap.* **2022**, *76*, 1271–1283. [CrossRef]
13. Lin, Y.; Yan, Y. Biosynthesis of caffeic acid in *Escherichia coli* using its endogenous hydroxylase complex. *Microb. Cell Factories* **2012**, *11*, 1–9. [CrossRef]
14. Huang, Q.; Lin, Y.; Yan, Y. Caffeic acid production enhancement by engineering a phenylalanine over-producing *Escherichia coli* strain. *Biotechnol. Bioeng.* **2013**, *110*, 3188–3196. [CrossRef] [PubMed]
15. Tošović, J. Spectroscopic features of caffeic acid: Theoretical study. *Kragujev. J. Sci.* **2017**, *39*, 99–108. [CrossRef]
16. Agunloye, O.M.; Oboh, G.; Ademiluyi, A.O.; Ademosun, A.O.; Akindahunsi, A.A.; Oyagbemi, A.A.; Omobowale, T.O.; Ajibade, T.O.; Adedapo, A.A. Cardio-protective and antioxidant properties of caffeic acid and chlorogenic acid: Mechanistic role of angiotensin converting enzyme, cholinesterase and arginase activities in cyclosporine induced hypertensive rats. *Biomed. Pharmacother.* **2019**, *109*, 450–458. [CrossRef] [PubMed]
17. Verma, R.P.; Hansch, C. An approach towards the quantitative structure–activity relationships of caffeic acid and its derivatives. *ChemBioChem* **2004**, *5*, 1188–1195. [CrossRef] [PubMed]
18. Rodrigues, J.; Araujo, R.G.; Prather, K.; Kluskens, L.; Rodrigues, L. Heterologous production of caffeic acid from tyrosine in *Escherichia coli*. *Enzym. Microb. Technol.* **2015**, *71*, 36–44. [CrossRef]

19. Sznitowska, M.; Janicki, S.; Dabrowska, E.A.; Gajewska, M. Physicochemical screening of antimicrobial agents as potential preservatives for submicron emulsions. *Eur. J. Pharm. Sci.* **2002**, *15*, 489–495. [[CrossRef](#)]
20. Xie, J.; Yang, F.; Zhang, M.; Lam, C.; Qiao, Y.; Xiao, J.; Zhang, D.; Ge, Y.; Fu, L.; Xie, D. Antiproliferative activity and SARs of caffeic acid esters with mono-substituted phenylethanols moiety. *Bioorganic Med. Chem. Lett.* **2017**, *27*, 131–134. [[CrossRef](#)]
21. Bispo, V.S.; Dantas, L.S.; Filho, A.D.B.C.; Pinto, I.F.; Da Silva, R.P.; Otsuka, F.A.M.; Santos, R.B.; Santos, A.C.; Trindade, D.J.; Matos, H.R. Reduction of the DNA damages, hepatoprotective effect and antioxidant potential of the coconut water, ascorbic and caffeic acids in oxidative stress mediated by ethanol. *An. Acad. Bras. Cienc.* **2017**, *89*, 1095–1109. [[CrossRef](#)] [[PubMed](#)]
22. Lee, K.W.; Kang, N.J.; Kim, J.H.; Lee, K.M.; Lee, D.E.; Hur, H.J.; Lee, H.J. Caffeic acid phenethyl ester inhibits invasion and expression of matrix metalloproteinase in SK-Hep1 human hepatocellular carcinoma cells by targeting nuclear factor kappa B. *Genes Nutr.* **2008**, *2*, 319–322. [[CrossRef](#)] [[PubMed](#)]
23. Won, C.; Lee, C.S.; Lee, J.-K.; Kim, T.-J.; Lee, K.-H.; Yang, Y.M.; Kim, Y.-N.; Ye, S.-K.; Chung, M.-H. CADPE suppresses cyclin D1 expression in hepatocellular carcinoma by blocking IL-6-induced STAT3 activation. *Anticancer Res.* **2010**, *30*, 481–488.
24. Gu, W.; Yang, Y.; Zhang, C.; Zhang, Y.; Chen, L.; Shen, J.; Li, G.; Li, Z.; Li, L.; Li, Y.; et al. Caffeic acid attenuates the angiogenic function of hepatocellular carcinoma cells via reduction in JNK-1-mediated HIF-1 α stabilization in hypoxia. *RSC Adv.* **2016**, *6*, 82774–82782. [[CrossRef](#)]
25. Phadke, A.V.; Tayade, A.A.; Khambete, M.P. Therapeutic potential of ferulic acid and its derivatives in Alzheimer's disease—A systematic review. *Chem. Biol. Drug Des.* **2021**, *98*, 713–721. [[CrossRef](#)] [[PubMed](#)]
26. Tee-Ngam, P.; Nunant, N.; Rattanarat, P.; Siangproh, W.; Chailapakul, O. Simple and rapid determination of ferulic acid levels in food and cosmetic samples using paper-based platforms. *Sensors* **2013**, *13*, 13039–13053. [[CrossRef](#)]
27. Balasubashini, M.S.; Rukkumani, R.; Viswanathan, P.; Menon, V.P. Ferulic acid alleviates lipid peroxidation in diabetic rats. *Phytother. Res.* **2004**, *18*, 310–314. [[CrossRef](#)]
28. Koh, P.-O. Ferulic acid prevents the cerebral ischemic injury-induced decreases of astrocytic phosphoprotein PEA-15 and its two phosphorylated forms. *Neurosci. Lett.* **2012**, *511*, 101–105. [[CrossRef](#)]
29. Koh, P.-O. Ferulic acid prevents the cerebral ischemic injury-induced decrease of Akt and Bad phosphorylation. *Neurosci. Lett.* **2012**, *507*, 156–160. [[CrossRef](#)]
30. Koh, P.-O. Ferulic acid attenuates the injury-induced decrease of protein phosphatase 2A subunit B in ischemic brain injury. *PLoS ONE* **2013**, *8*, e54217.
31. Cheng, C.Y.; Su, S.Y.; Tang, N.Y.; Ho, T.Y.; Lo, W.Y.; Hsieh, C.L. Ferulic acid inhibits nitric oxide-induced apoptosis by enhancing GABA B1 receptor expression in transient focal cerebral ischemia in rats. *Acta Pharmacol. Sin.* **2010**, *31*, 889–899. [[CrossRef](#)] [[PubMed](#)]
32. Kim, H.-Y.; Lee, S.-M. Ferulic acid attenuates ischemia/reperfusion-induced hepatocyte apoptosis via inhibition of JNK activation. *Eur. J. Pharm. Sci.* **2012**, *45*, 708–715. [[CrossRef](#)] [[PubMed](#)]
33. Baskaran, N.; Manoharan, S.; Balakrishnan, S.; Pugalandhi, P. Chemopreventive potential of ferulic acid in 7, 12-dimethylbenz [a] anthracene-induced mammary carcinogenesis in Sprague–Dawley rats. *Eur. J. Pharmacol.* **2010**, *637*, 22–29. [[CrossRef](#)] [[PubMed](#)]
34. Manoharan, S.; Rajasekaran, D.; Prabhakar, M.; Karthikeyan, S.; Manimaran, A. Anti-cell proliferative efficacy of ferulic acid against 7, 12-dimethylbenz (a) anthracene induced hamster buccal pouch carcinogenesis. *Asian Pac. J. Cancer Prev.* **2012**, *13*, 5207–5211. [[CrossRef](#)] [[PubMed](#)]
35. Wang, T.; Gong, X.; Jiang, R.; Li, H.; Du, W.; Kuang, G. Ferulic acid inhibits proliferation and promotes apoptosis via blockage of PI3K/Akt pathway in osteosarcoma cell. *Am. J. Transl. Res.* **2016**, *8*, 968.
36. Kiokias, S.; Oreopoulou, V. A Review of the Health Protective Effects of Phenolic Acids against a Range of Severe Pathologic Conditions (Including Coronavirus-Based Infections). *Molecules* **2021**, *26*, 5405. [[CrossRef](#)]
37. Hiorcea-Paquim, A.; Enache, T.A.; De Souza Gil, E.; Oliveira-Brett, A.M. Natural phenolic antioxidants electrochemistry: Towards a new food science methodology. *Compr. Rev. Food Sci. Food Saf.* **2020**, *19*, 1680–1726. [[CrossRef](#)]
38. Zeb, A. Concept, mechanism, and applications of phenolic antioxidants in foods. *J. Food Biochem.* **2020**, *44*, e13394. [[CrossRef](#)]
39. Sato, Y.; Itagaki, S.; Kurokawa, T.; Ogura, J.; Kobayashi, M.; Hirano, T.; Sugawara, M.; Iseki, K. In vitro and in vivo antioxidant properties of chlorogenic acid and caffeic acid. *Int. J. Pharm.* **2011**, *403*, 136–138. [[CrossRef](#)]
40. Zduńska, K.; Dana, A.; Kolodziejczak, A.; Rotsztein, H. Antioxidant properties of ferulic acid and its possible application. *Ski. Pharmacol. Physiol.* **2018**, *31*, 332–336. [[CrossRef](#)]
41. Kiani, R.; Arzani, A.; Maibody, S.M. Polyphenols, flavonoids, and antioxidant activity involved in salt tolerance in wheat, *Aegilops cylindrica* and their amphidiploids. *Front. Plant Sci.* **2021**, *12*, 493. [[CrossRef](#)] [[PubMed](#)]
42. Magnani, C.; Isaac, V.L.B.; Correa, M.A.; Salgado, H.R.N. Caffeic acid: A review of its potential use in medications and cosmetics. *Anal. Methods* **2014**, *6*, 3203–3210. [[CrossRef](#)]
43. Chan, W.-S.; Wen, P.-C.; Chiang, H.-C. Structure-activity relationship of caffeic acid analogues on xanthine oxidase inhibition. *Anticancer Res.* **1995**, *15*, 703–707. [[PubMed](#)]
44. Son, S.; Lewis, B.A. Free radical scavenging and antioxidative activity of caffeic acid amide and ester analogues: Structure—Activity relationship. *J. Agric. Food Chem.* **2002**, *50*, 468–472. [[CrossRef](#)]
45. Naumowicz, M.; Kusaczuk, M.; Zajac, M.; Jabłońska-Trypuć, A.; Mikłosz, A.; Gál, M.; Worobiczuk, M.; Kotyńska, J. The influence of the pH on the incorporation of caffeic acid into biomimetic membranes and cancer cells. *Sci. Rep.* **2022**, *12*, 1–15. [[CrossRef](#)]

46. Chang, W.-C.; Hsieh, C.-H.; Hsiao, M.-W.; Lin, W.-C.; Hung, Y.-C.; Ye, J.-C. Caffeic acid induces apoptosis in human cervical cancer cells through the mitochondrial pathway. *Taiwan J. Obstet. Gynecol.* **2010**, *49*, 419–424. [[CrossRef](#)]
47. Hung, M.-W.; Shiao, M.-S.; Tsai, L.-C.; Chang, G.-G.; Chang, T.-C. Apoptotic effect of caffeic acid phenethyl ester and its ester and amide analogues in human cervical cancer ME180 cells. *Anticancer Res.* **2003**, *23*, 4773–4780.
48. Min, J.; Shen, H.; Xi, W.; Wang, Q.; Yin, L.; Zhang, Y.; Yu, Y.; Yang, Q.; Wang, Z.-N. Synergistic anticancer activity of combined use of caffeic acid with paclitaxel enhances apoptosis of non-small-cell lung cancer H1299 cells in vivo and in vitro. *Cell. Physiol. Biochem.* **2018**, *48*, 1433–1442. [[CrossRef](#)]
49. Espíndola, K.M.M.; Ferreira, R.G.; Narvaez, L.E.M.; Rosario, A.C.R.S.; Da Silva, A.H.M.; Silva, A.G.B.; Vieira, A.P.O.; Monteiro, M.C. Chemical and pharmacological aspects of caffeic acid and its activity in hepatocarcinoma. *Front. Oncol.* **2019**, *9*, 541. [[CrossRef](#)]
50. Nakatani, N.; Kayano, S.I.; Kikuzaki, H.; Sumino, K.; Katagiri, K.; Mitani, T. Identification, quantitative determination, and antioxidative activities of chlorogenic acid isomers in prune (*Prunus domestica* L.). *J. Agric. Food Chem.* **2000**, *48*, 5512–5516. [[CrossRef](#)]
51. Bunzel, M.; Ralph, J.; Funk, C.; Steinhart, H. Structural elucidation of new ferulic acid-containing phenolic dimers and trimers isolated from maize bran. *Tetrahedron Lett.* **2005**, *46*, 5845–5850. [[CrossRef](#)]
52. Mysliwiec, A.G.; Ornstein, D.L. Matrix metalloproteinases in colorectal cancer. *Clin. Colorectal Cancer* **2002**, *1*, 208–219. [[CrossRef](#)] [[PubMed](#)]
53. Dodurga, Y.; Eroğlu, C.; Seçme, M.; Elmas, L.; Avcı, Ç.B.; Şatıroğlu-Tufan, N.L. Anti-proliferative and anti-invasive effects of ferulic acid in TT medullary thyroid cancer cells interacting with URG4/URGCP. *Tumor Biol.* **2016**, *37*, 1933–1940. [[CrossRef](#)]
54. Klassen, L.; Chequin, A.; Manica, G.; Biembengut, I.V.; Toledo, M.B.; Baura, V.A.; Pedrosa, F.D.O.; Ramos, E.; Costa, F.F.; de Souza, E.M.; et al. MMP9 gene expression regulation by intragenic epigenetic modifications in breast cancer. *Gene* **2018**, *642*, 461–466. [[CrossRef](#)] [[PubMed](#)]
55. Wu, S.; Zheng, Q.; Xing, X.; Dong, Y.; Wang, Y.; You, Y.; Chen, R.; Hu, C.; Chen, J.; Gao, D.; et al. Matrix stiffness-upregulated LOXL2 promotes fibronectin production, MMP9 and CXCL12 expression and BMDCs recruitment to assist pre-metastatic niche formation. *J. Exp. Clin. Cancer Res. CR* **2018**, *37*, 99. [[CrossRef](#)]
56. Aborehab, N.M.; Elnagar, M.R.; Waly, N.E. Gallic acid potentiates the apoptotic effect of paclitaxel and carboplatin via over-expression of Bax and P53 on the MCF-7 human breast cancer cell line. *J. Biochem. Mol. Toxicol.* **2021**, *35*, e22638. [[CrossRef](#)] [[PubMed](#)]